Gas Chromatographic Behavior of Poly(vinyl acetate) at Temperatures Encompassing T_g: Determination of T_g and χ

D. D. Deshpande* and O. S. Tyagi

Department of Chemistry, Indian Institute of Technology, Powai, Bombay-400 076, India.
Received November 29, 1977

ABSTRACT: Using poly(vinyl acetate) as the stationary liquid phase in the GLC column, retention data are obtained for various hydrocarbons, carbon tetrachloride, and chloroform as probes at different flow rates and various temperatures encompassing the glass transition temperature T_g. The nature of the flow diagram depends on the probe and the column temperature. Such detailed studies are required to obtain flow rate independent V^0_g to be used in the calculation of the thermodynamic interaction parameter χ. For the PVAc–probe system, generally a temperature higher than 80 °C is required in order to reach a true thermodynamic sorption equilibrium. The glass transition temperature T_g could be estimated from the retention diagram but the reliability of such estimations depends on the specific probe used.

The gas liquid chromatographic (GLC) technique has been widely used nowadays for studying the polymer–solvent interaction parameter.[1–11] The observations of Smidsrod and Guillet[12] on the change in the slope (inversion) of the retention curve (retention diagram) obtained by plotting the logarithm of the specific retention volume (V^0_g) vs. reciprocal of the absolute temperature have revealed the possibility of estimating the glass transition temperature (T_g) of polymer stationary phases using the GLC or "molecular probe" technique.[9,10,12–22] In addition, the retention diagram can provide useful information on the degree of crystallinity,[13,22,23] melting transitions,[18,24] crystallization kinetics,[25] diffusion coefficients,[26] and various surface properties.[27,28] A detailed examination of such a retention diagram indicates that its nature depends strongly on the solute (probe) used and that it may often be divided into three distinct regions as shown in Figure 1. Region I corresponds to equilibrium surface adsorption and region III to equilibrium sorption, while region II corresponds to nonequilibrium sorption.

The inversion in the retention curve occurs due to a change in retention mechanism. For the concurrent retention mechanisms encountered with polymers in the vicinity of T_g, the net retention volume V_R is given by the relation[29]

$$V_R = K_b W_L + K_a A_L \qquad (1)$$

where K_b and K_a are the partition coefficients for bulk sorption and surface adsorption and W_L and A_L are the mass and surface area of the stationary phase. At temperatures below T_g, the second term in eq 1 will dominate, while at temperatures far above T_g the relative contribution of the first term will be far greater than that of the second term. The ability of the probe to cause a sharp inversion lies in its ability to penetrate into polymer bulk just above T_g. This, in turn, is a function of size and shape of the probe molecule, the nature of its interaction with the polymer, the structure and thickness of the polymer film on the support surface,[9,19,20] polymer stereoregularity,[17,24] and other kinetic parameters which affect the shape of elution peaks[30] and also the porosity of the polymer sample if it is packed into GLC column without a support.[14] The probe sample size and residence time in the column also influence the inversion at T_g. The latter depends on the flow rate of the carrier gas.

True thermodynamic interaction parameters can be evaluated only if the equilibrium sorption condition is established, viz., one should ensure that GLC data are obtained in region III of Figure 1. It does, therefore, become imperative to investigate the onset temperature for region III.

In this work poly(vinyl acetate) (PVAc) has been utilized as stationary liquid phase. The results of earlier workers[31,32] on PVAc vary widely, V^0_g reported differing by 32–57%. Selecting any one of the values for calculation of thermodynamic interaction parameter is, therefore, questionable. PVAc has a polar surface for adsorption and has a wide range of solubilities for various organic solvents which make it a promising stationary phase for gas chromatographic studies near glass transition temperature. The results on various probes and at various flow rates have been given here at different temperatures encompassing the glass transition region.

Experimental Section

The poly(vinyl acetate) used was a BDH product No. 30572 ($\bar{M}_v$ = 40 000 and $\bar{M}_n$ = 6 700). The polymer was deposited onto Chromosorb P (AW, 80–100 mesh) from benzene solution by continuous stirring and slow evaporation of benzene at 50 °C under partial vacuum. The coated support was dried in a vacuum oven at 50 °C and 5 Torr for 48 h and sieved. All columns were prepared from 0.25 in. o.d. annealed copper tubing. The column loading was determined by calcination. Following Braun et al.,[33] loss of volatile matter from the support during heat treatment was determined by calcination of uncoated support under identical conditions and was found to be 0.1751%; the correction was applied accordingly.

The nine probes used were *n*-hexane, *n*-heptane, *n*-octane, isooctane, cyclohexane, carbon tetrachloride, chloroform, benzene, and toluene. They were all analytical grade chemicals used after fractional distillation.

A dual column GLC apparatus with precise temperature and pressure regulation was assembled using a four-filament thermal conductivity detector. The columns were housed in a liquid thermostat regulated to ±0.05 °C. Hydrogen was used as carrier gas. The flow rates were measured with a soap bubble flow meter at the detector outlet. The method of Tewari et al.[34] was adopted for introduction of probes onto column head as an infinitely sharp vapor-phase front. The injector temperature was kept between 100 and 120 °C to facilitate flash vaporization of liquid probe before its entry into the column. The detector temperature was 170 °C. A minimum of three consecutive injections were made for each probe at every flow rate studied, and an average of these retention times was used to calculate V^0_g. The accuracy in such V^0_g values at a given flow rate was within 1%. In the flow rate independent region, when V^0_g is required for calculation of the χ parameter, an average of V^0_g values obtained at different flow rates was used. These averaged values are given in Table III along with mean deviation for each probe. In general the deviation was ±1%. The corresponding uncertainty in χ is also reported in Table III.

The GLC apparatus and the method were verified using squalane. The data were in agreement with literature[35–38] within 1.1 to 1.8%.

Data Treatment

The specific retention volumes (V^0_g) corrected to 0 °C were calculated from the corrected retention times using the following expression[39]

$$V^0_g = t_R \frac{F}{W_L} \frac{P_o - p_w}{P_o} \frac{273.2}{T_a} \frac{3}{2} \frac{(P_i/P_o)^2 - 1}{(P_i/P_o)^3 - 1} \qquad (2)$$

where t_R is the net retention time, F is the carrier gas flow rate measured at room temperature T_a, W_L is the weight of stationary phase in the column, P_i and P_o are inlet and outlet

0024-9297/78/2211-0746$01.00/0

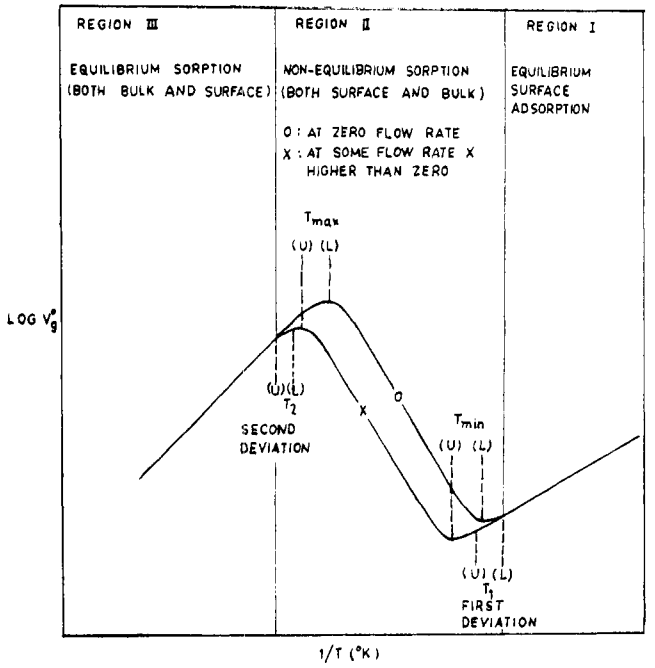

Figure 1. Typical retention diagram through T_g of polymer stationary phases. Effect of carrier gas flow rates.

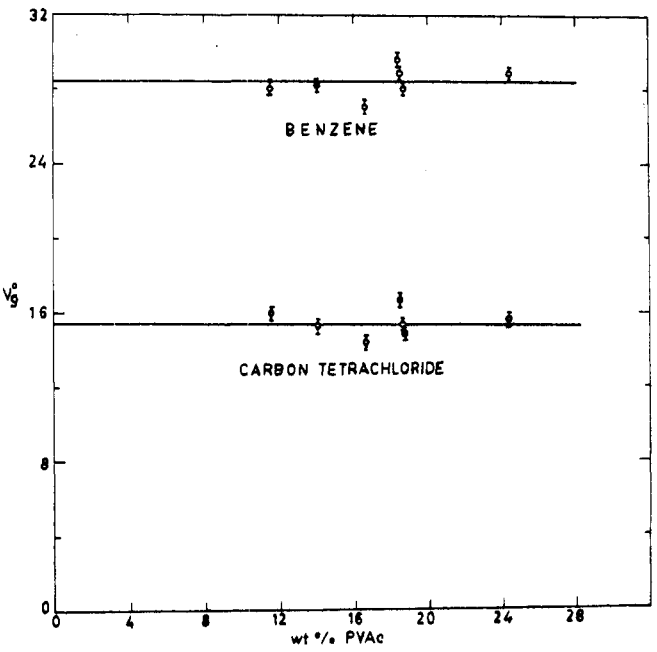

Figure 2. Effect of PVAc coating on specific retention volumes of benzene and carbon tetrachloride at 100.0 °C and 73.2 mL/min flow rate.

pressures, respectively, and p_w is water vapor pressure at temperature T_a.

The thermodynamic interaction parameters χ were calculated from the following relation[1] using Flory–Huggins (lattice) approximation to polymer solutions

$$\chi = \ln \frac{273.2Rv_2}{V^0_g V_1 P_1^0} - \left(1 - \frac{V_1}{M_2 v_2}\right) - \frac{P_1^0}{RT}(B_{11} - V_1) \quad (3)$$

where V_1 is the liquid state molar volume of solute, P_1^0 is its vapor pressure at column temperature T °K, v_2 is the specific volume of polymer, B_{11} is the gas state second virial coefficient of the solute, M_2 is the molecular weight of the polymer, R is the gas constant, and χ is the Flory–Huggins interaction parameter.

B_{11} and P_1^0 were computed from the modified corresponding states equation of McGlashan and Potter[40] and from the Antoine equation respectively using constants from Dreisbach's compilation.[41] v_2 was obtained from the density data.[42]

Table I
Column Parameters for Poly(vinyl acetate) Stationary Phases

Column No.	Length, cm	Loading, wt %	Packing, g	Mass of stationary phase, g
1	84	11.516	7.487	0.8622
2	84	13.963	7.679	1.0722
3	84	16.566	7.963	1.3191
4	122	18.418	12.557	2.3127
5	84	18.449	8.068	1.4885
6	61	18.588	6.116	1.1369
7	115	24.468	12.593	3.0812

Results and Discussion[45]

Effect of Column Loading. In order to determine optimum loading of stationary phase, seven columns were prepared in the range of 11.5 to 24.5% loading. The details of these columns are described in Table I. Two probes, viz., benzene and carbon tetrachloride, were investigated at a flow rate of 73.2 mL/min and at a temperature of 100 °C, sufficiently higher than the glass transition temperature T_g of PVAc (literature value of 32 °C).[43] The retention volumes are shown in Figure 2 and reveal constancy of the data within the experimental limits. Data on detailed investigations using various probes, and as a function of temperature and of flow rate reported here, were taken on one of these columns (column no. 4).

Newman and Prausnitz[31] and Lichtenthaler et al.[32] have reported retention volumes V^0_g at 100 °C for benzene, toluene, and chloroform using PVAc as the stationary phase. Our data agree within 4% with those reported by Lichtenthaler et al. Data of Newman and Prausnitz are however higher by an average of 36.4% from our data. These authors have used peak maximum point to calculate t_R while we have used the method of tangents at ⅔ peak height to obtain t_R which gives 2% lower values of V^0_g.

Effect of Probe Sample Size. At temperatures below 45 °C, the retention time at peak maximum (t_R) was small compared to the peak broadening. A probe sample size less than 0.05 μL could not produce convenient peak profiles for measurement of t_R at infinite dilution of vapors in polymer, particularly in the case of n-octane, toluene, and chloroform. This was a result of the decrease in the number of probe moles eluting in the sharp pulse portion of the peak and their increase in the tail because the kinetic factor is decreased in slow bulk equilibration.[30] Typical peaks for the surface adsorption region were obtained in an effort to get reliable values of t_R using peaks of sufficient height and having larger elution near peak maximum obtainable by introducing larger samples of probes. The asymmetric peak fronts were observed for n-octane below 29 °C and for toluene up to as high as 37.5 °C. This gave an indication of dependence of t_R on probe sample size. This, however, was not studied quantitatively. The increase in asymmetry with sample size defied the attempt to obtain reliable values of t_R in this way with n-octane and toluene. At temperatures higher than 80 °C, t_R could be determined at effectively infinite dilution of probe in the polymer.

Effect of Flow Rates at Various Temperatures. True bulk retention volumes were obtained by Lichtenthaler et al.[32] and Braun and Guillet[19] by extrapolation to zero flow rate from the measurements at low flow rates. At very low flow rates the experimental uncertainty increases.

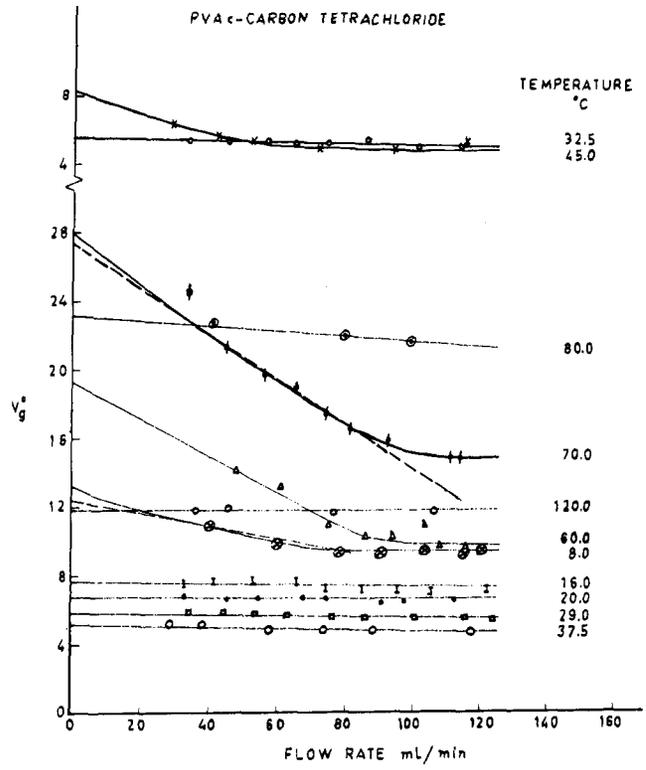

Figure 3. Effect of flow rate on V^0_g of carbon tetrachloride on PVAc.

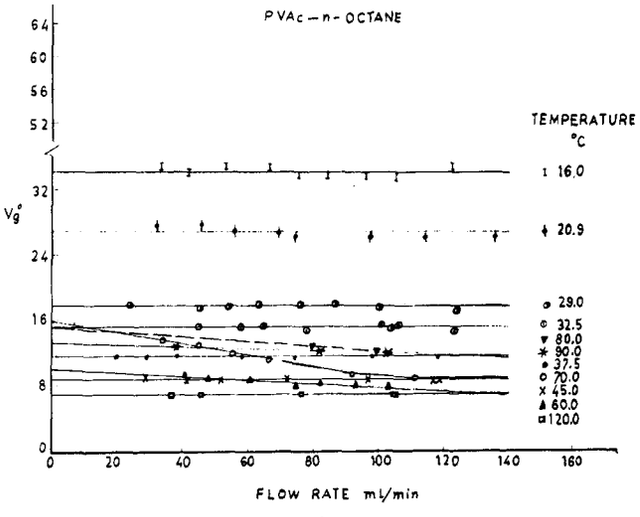

Figure 4. Effect of flow rate on V^0_g of *n*-octane on PVAc.

The experimental observations of variation of V^0_g with flow rate (F) are given in Figures 3 and 4 for some representative probes and at some selected temperatures. The present studies indicate that in general the dependence of V^0_g on F can be represented by Figure 5 consisting of three regions. Region I observed as a plateau in the flow diagrams is generally detectable at $F > 70$ mL/min. Region III consists of a near-linear dependence of V^0_g on F, while in region II the linear dependence of region III asymptotically approaches the plateau, and V^0_g is very sensitive to slight change in F (in the range F(L) to F(U)). Hence region II, where the retention volume is strongly dependent on kinetic factors, is described here as the "flow transition". Its position depends on the probe used and on the column temperature. For this purpose, some characteristic temperatures, T_1, T_2, T_{min}, and T_{max}, are defined as shown in Figure 1, which is also a general representation of typical retention curves (Figures 6 and 7) obtained using interpolated and extrapolated values of V^0_g from flow diagrams. T_1 and T_2 are the first and second deviations from linearity respectively in regions I and II of Figure 1, and T_{min} and T_{max} are two inversion points corresponding to minimum and maximum respectively in region II. The letter L indicates the values at zero flow rate (extrapolated) and U at a flow rate of 120 mL/min in region I of Figure 5. These characteristic temperatures obtained graphically from retention diagrams are given in Table II, and in terms of these, the shift of the position of the "flow transition" in the flow diagrams can be summarized as follows:

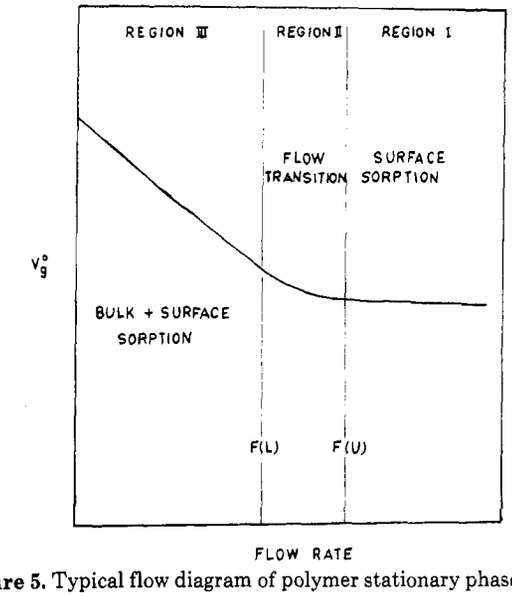

Figure 5. Typical flow diagram of polymer stationary phases.

a. For the plateau region, V^0_g is independent of F in the entire region of 0 to 120 mL/min if the temperature is below T_1(L).

b. V^0_g varies linearly with F in the temperature range of T_1(L) and T_{min} (U). The largest slope is shown by chloroform followed by toluene, benzene, and carbon tetrachloride. The reasons for such variations are probably the strong H-bonding and specific interaction tendencies of these probes further favored by increase in residence time at low flow rates.

c. There is considerable nonlinear increase in V^0_g on decreasing flow rates between temperatures T_{min}(U) and T_{max}(U). Nonlinearity in flow diagrams appears first at T_{min}(U) in most of the cases. The "flow transition" region shifts to a higher value of F if the temperature is increased to T_{max}(U) and ultimately disappears. The flow rate coefficient of V^0_g also increases with temperature in both regions II and III of Figure 5.

d. If the temperature is increased further above T_{max}(U) (or T_{max}(L) in some cases), the near-linear dependence of V^0_g on F is observed. The slope of V^0_g vs. F diminishes with increase of temperature and again a flow rate independence is observed above T_2(U). Except in the vicinity of 70 °C, alkane probes show linear dependence of V^0_g on F at all the temperatures studied (see Figure 4).

e. Flow diagrams at temperatures below 16 °C show scattered values of V^0_g possibly due to very low vapor pressures of the probe and by peak asymmetry and broadening which is large compared to t_R. Some alkane probes show the scattering even at 20.9 °C though to a small extent. There is no scattering of data points on V^0_g even at 8.0 °C in the case of carbon tetrachloride and the flow diagram is similar to those obtained between T_{min}(U) and T_{max}(L) (Figure 3).

All the experimentally obtained flow diagrams can be considered as a result of the extension either of plateau region

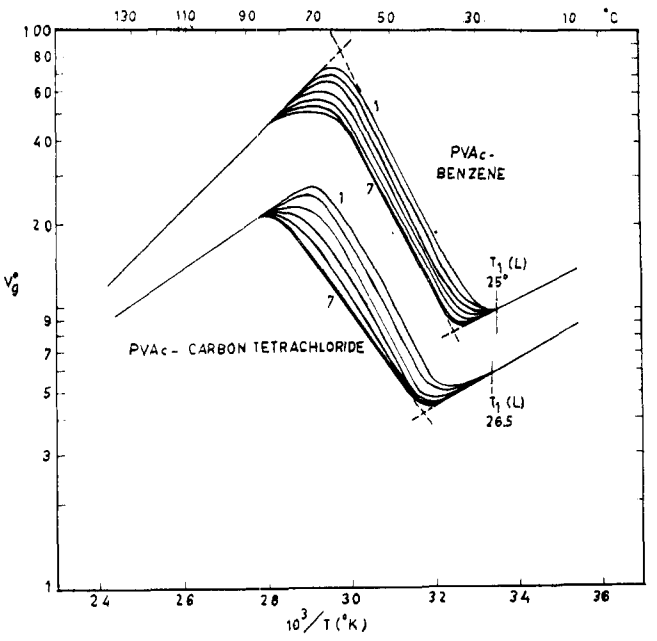

Figure 6. Retention diagram for benzene and carbon tetrachloride probes on PVAc at flow rates (extrapolated) zero (1), 20 (2), 40 (3), 60 (4), 80 (5), 100 (6), and 120 (7) mL/min.

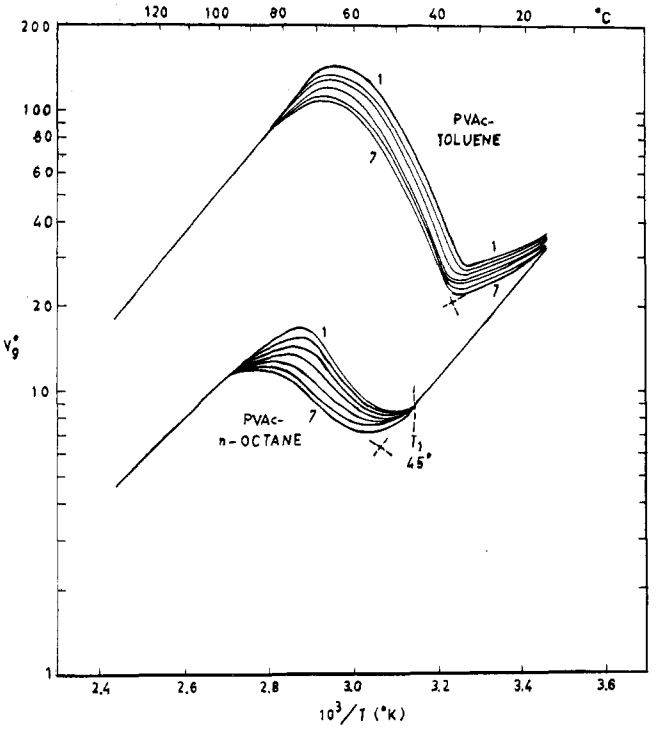

Figure 7. Retention diagram for *n*-octane and toluene probes on PVAc at different flow rates. The numbers correspond to those in Figure 6.

I (surface adsorption partition retention mechanism) to lower flow rates or of near-linear region III (bulk equilibrium partition retention mechanism) to higher flow rates.

In view of these observations, the flow diagrams at temperatures below T_1(L) become an experimental proof for the proposition of Courval and Gray[30] that surface adsorption equilibrium is an instantaneous process, an assumption made by them while computing peak shapes from kinetic parameters near T_g.

Retention Diagrams. At temperatures below T_g, the retention is essentially surface adsorption (region I of Figure 2). At temperature T_g or above T_g (region II) the deviation from linearity is due to the onset of penetration of probe molecules into the polymer phase as a result of increasing mobility of the polymer chain segments observable as the first deviation at T_1. Inversion in the slope of retention curve, that is inversion in the temperature coefficient of V^0_g, occurs at temperature T_{min}. The contribution due to bulk partition retention (first term in eq 1) to the net retention volume increases from T_1 to T_{max}. Above T_{max} normal laws of GLC are observed by the polymer stationary phase, and a second inversion in the temperature coefficient of V^0_g occurs. The bulk component of retention volume predominates above temperature T_2 corresponding to a "second deviation" from linearity in region III. In region II, described as the nonequilibrium region, the retention is mostly governed by kinetic factors although contributions from other sources cannot be ignored. The temperatures T_1, T_{min}, T_{max}, and T_2 are dependent on factors causing shifts in retention diagrams, the most important of which are coating thickness[9,19,20] and flow rate. These temperatures should therefore be identified as characteristic temperatures for a given polymer–probe system under the given experimental conditions. In addition, the size and nature of the probe molecule[16] and polymer–probe interactions (and eventually the solubility)[12,44] also determine the shape of retention diagrams. Sharpness of deviation at T_1 is related qualitatively to the ratio V^0_g/U_s, where U_s is the surface adsorption retention volume (ref 10), which depends on the extent of bulk sorption just above T_g, and is reflected in the closeness of T_1(L) and T_{min}(U). The present work shows that inversion in retention diagram occurs at temperatures even higher than T_g where the ratio V^0_g/U_s becomes greater than unity in the case of poor solvents like *n*-octane (Figure 7). In the case of toluene on the other hand, no T_1 is observed down to 16 °C (Figure 7). The onset of bulk equilibrium sorption takes place at temperature T_2.

Estimation of T_g. The glass transition of PVAc is reported to be in the range of 28 to 32 °C.[42,43] The gas chromatographically determined value of T_g (corresponding to T_{min}) is reported to be 40 °C.[15a] The T_1(L) values reported in Table II are very close to the literature value of T_g except for *n*-octane and toluene probes. In the case of *n*-octane a sharp

Table II
Characteristic Temperatures[a] (°C) Obtained from Retention Diagrams for Poly(vinyl acetate)–Probe Systems on Column No. 4

Probe	T_1(L)	T_1(U)	T_{min}(L)	T_{min}(U)	T_{max}(L)	T_{max}(U)	T_2(L)	T_2(U)
n-Octane	45	45	50	58	76	87	92	97
Isooctane	29–37.5[b]	37–49[b]	62	69	98	100	110[b]	≥120[b]
Cyclohexane	21[b]	39	42	46	85	93	100[b]	120
Carbon tetrachloride	26	39	36	42	68	84	84	86
Benzene	25	33	28	35	63	70	70	83
Toluene		<16[b]	32	36	60	70	72	87
Chloroform	23	32	23	32	59	70	69	87

[a] Uncertainty in estimation is ±1 °C. [b] The changes in the retention diagrams were not distinct in these cases.

Table III
Specific Retention Volumes and Interaction Parameters for PVAc–Probe Systems at Selected Temperatures above T_2(L)

Probe	120.0 °C V^0_g	Max deviation ±	Max deviation %	χ	Uncertainty in χ	100.0 °C V^0_g	Max deviation ±	Max deviation %	χ	Uncertainty in χ
n-Hexane	2.48	0.06	2.42	1.709	0.024	3.29	0.06	1.83	1.933	0.018
n-Heptane	4.18	0.10	2.40	1.815	0.024	5.97	0.14	2.35	2.036	0.023
n-Octane	6.96	0.08	1.15	1.935	0.012	10.80	0.09	0.79	2.143	0.008
Isooctane	3.76	0.16	4.25	1.862	0.042	4.84	0.12	2.38	2.167	0.025
Cyclohexane	5.82	0.14	2.32	1.311	0.033	7.75	0.03	0.32	1.564	0.004
Carbon tetrachloride	11.86	0.09	0.76	0.630	0.007	18.46	0.41	2.22	0.714	0.022
Benzene	18.87	0.11	0.60	0.280	0.005	30.87	0.22	0.71	0.339	0.008
Toluene	30.97	0.31	1.00	0.458	0.011	53.67	0.47	0.88	0.513	0.009
Chloroform	21.56	0.22	1.02	−0.076	0.010	36.10	0.00	0.00	−0.109	0.000
Mean deviation		0.14	1.77		0.019		0.17	1.28		0.013

Probe	90.0 °C V^0_g	Max deviation ±	Max deviation %	χ	Uncertainty in χ	80.0 °C V^0_g	χ
n-Octane	13.4[a]			2.262			
Carbon tetrachloride	20.98	0.33	1.57	0.853	0.016		
Benzene	38.96	0.14	0.36	0.386	0.004	49.48[a]	0.445
Toluene	70.31	0.07	1.00	0.557	0.009	97.15[a]	0.562
Chloroform	46.79	0.17	0.35	−0.124	0.003	63.49	−0.168
Mean deviation		0.18	0.82		0.008		

[a] Extrapolated values of V^0_g to zero flow rate.

deviation occurs at 45 °C (T_1(L) as well as T_1(U)), a temperature higher than T_g (Figure 7). Most probably, *n*-octane having a large size cannot diffuse into the bulk of PVAc until sufficient segmental mobility is achieved by PVAc chains, and a higher value of T_g is thus observed. On the other hand, in the case of toluene, no sharp deviation could be observed experimentally due to peak broadening and peak asymmetry on the front profile, the shape of which corresponded to an anti-Langmuir type solubility isotherm. These peak shape problems resulted in scattered experimental points at temperatures 16 °C and below. No generalization could be made about the capability of a probe in terms of its solubility in polymer, molecular weight, or size to effectively detect T_g through observed sharp deviation (T_1) in the retention diagram. In this regard there is no agreement among the earlier workers.[1,12,16] The sharpness of deviation at T_1 decreases in the order chloroform, benzene, carbon tetrachloride, and alkanes. Estimation of T_g using carbon tetrachloride is more reliable than using alkanes, probably due to its swelling action on PVAc.[42]

Interaction Parameter. The thermodynamically controlled true retention volumes V^0_g, independent of flow rates, were obtained above temperatures 100 °C for alkanes and 80 °C for other probes. The data given in Table III are an average of various flow rates studied. V^0_g extrapolated to zero flow rate were used wherever necessary, and this is indicated in Table III. The thermodynamic interaction parameters χ calculated using these data are also given in Table III. For normal alkanes they increase with chain length. For aromatic hydrocarbons and carbon tetrachloride the magnitude of χ is much less than that for alkanes. The π electrons in aromatic hydrocarbons, and specific polymer–probe interactions in the case of carbon tetrachloride, are responsible for low values of χ. When the solute–solvent interaction is very strong due to H bonding, the χ parameter becomes negative as in the case of chloroform. The appreciable increase in the χ parameter with decrease in temperature shows the decrease in polymer–probe compatibility.

Conclusion

The thermodynamic interaction parameter for the polymer–probe system can be calculated from the flow rate independent retention volume V^0_g measured at temperatures sufficiently higher than T_g. The detailed studies on flow rate dependence of V^0_g reveal that the flow diagrams for a given probe depend on the column temperature used. Depending on the temperature, there is a shift of the "flow transition" region. Data on V^0_g collected in the "flow transition" region cannot be linearly extrapolated to obtain zero flow rate retention volume. From the retention diagram, it is possible to estimate the glass transition temperature T_g and it is found to occur at temperature T_1(L), the first deviation in the retention diagram. Since alkane probes do not show a sharp deviation, T_g estimation is less reliable in such cases. No generalizations could be made on the relationship of reliable estimations of T_g and the nature of probe or its solubility in the stationary phase.

Supplementary Material: Flow diagrams for benzene, toluene, chloroform, isooctane, and cyclohexane (8 pages). Ordering information can be found on any current masthead page.

References and Notes

(1) D. Patterson, Y. B. Tewari, H. P. Schreiber, and J. E. Guillet, *Macromolecules*, **4**, 356 (1971).
(2) W. R. Summers, Y. B. Tewari, and H. P. Schreiber, *Macromolecules*, **5**, 12 (1972).
(3) F. H. Covitz and J. W. King, *J. Polym. Sci., Part A-1*, **10**, 689 (1972).
(4) Y. B. Tewari and H. P. Schreiber, *Macromolecules*, **5**, 329 (1972).
(5) R. D. Newman and J. M. Prausnitz, *J. Polym. Sci., Part A-1*, **10**, 1492 (1972).
(6) H. P. Schreiber, Y. B. Tewari, and D. Patterson, *J. Polym. Sci., Part A-2*, **11**, 15 (1973).
(7) D. D. Deshpande, D. Patterson, H. P. Schreiber, and C. S. Su, *Macromolecules*, **7**, 530 (1974).
(8) O. Olabisi, *Macromolecules*, **8**, 316 (1975).
(9) Yu. S. Lipatov and A. E. Nesterov, *Macromolecules*, **8**, 889 (1975).
(10) J. M. Braun and J. E. Guillet, *Macromolecules*, **9**, 340 (1976).
(11) C. S. Su and D. Patterson, *Macromolecules*, **10**, 708 (1977).
(12) O. Smidsrod and J. E. Guillet, *Macromolecules*, **2**, 272 (1969).
(13) A. Lavoie and J. E. Guillet, *Macromolecules*, **2**, 443 (1969).
(14) J. R. Wallace, P. J. Kozak, and F. Noel, *SPE J.*, **26**, 43 (July 1970).

(15) (a) I. A. Schneider and E. M. Calugaru, *Eur. Polym. J.*, **10**, 729 (1974); (b) *ibid.*, **11**, 857 (1975); and (c) *ibid.*, **11**, 861 (1975).
(16) P. L. Hsiung and D. M. Cates, *J. Appl. Polym. Sci.*, **19**, 3051 (1975).
(17) J. M. Braun, A. Lavoie, and J. E. Guillet, *Macromolecules*, **8**, 311 (1975).
(18) G. J. Courval and D. G. Gray, *Macromolecules*, **8**, 326 (1975).
(19) J. M. Braun and J. E. Guillet, *Macromolecules*, **8**, 882 (1975).
(20) G. J. Courval and D. G. Gray, *Can. J. Chem.*, **54**, 3496 (1976).
(21) J. M. Braun and J. E. Guillet, *J. Polym. Sci., Polym. Chem. Ed.*, **14**, 1073 (1976).
(22) J. M. Braun and J. E. Guillet, *Macromolecules*, **9**, 617 (1976).
(23) J. M. Braun and J. E. Guillet, *Macromolecules*, **10**, 101 (1977).
(24) S. Galassi and G. Audisio, *Makromol. Chem.*, **175**, 2975 (1974).
(25) D. G. Gray and J. E. Guillet, *Macromolecules*, **4**, 129 (1971).
(26) D. G. Gray and J. E. Guillet, *Macromolecules*, **6**, 223 (1973).
(27) D. G. Gray and J. E. Guillet, *Macromolecules*, **5**, 316 (1972).
(28) B. Chabert, J. P. Soulier, and G. Edel, *Ann. Chim.*, **5**, 193 (1970).
(29) R. L. Martin, *Anal. Chem.*, **33**, 347 (1961).
(30) G. Courval and D. G. Gray, *Macromolecules*, **8**, 916 (1975).
(31) R. D. Newman and J. M. Prausnitz, *J. Paint Technol.*, **45**, 33 (1973).
(32) R. N. Lichtenthaler, D. D. Liu, and J. M. Prausnitz, *Macromolecules*, **7**, 565 (1974).
(33) J. M. Braun, M. Cutazar, J. E. Guillet, H. P. Schreiber, and D. Patterson, *Macromolecules*, **10**, 864 (1977).
(34) Y. B. Tewari, D. E. Martire, and J. P. Sheridan, *J. Phys. Chem.*, **74**, 2345 (1970).
(35) D. E. Martire and L. Z. Pollara, *J. Chem. Eng. Data*, **10**, 40 (1965).
(36) D. E. Martire, R. L. Pecsok, and J. H. Purnell, *Trans. Faraday Soc.*, **61**, 2496 (1965).
(37) A. J. B. Cruickshank, M. L. Windsor, and C. L. Young, *Proc. R. Soc. London, Ser. A*, **295**, 259 (1966); **295**, 271 (1966).
(38) E. C. Pease and S. Thorburn, *J. Chromatogr.*, **30**, 344 (1967).
(39) A. B. Littlewood, C. S. G. Phillips, and D. T. Price, *J. Chem. Soc.*, 1480 (1955).
(40) M. L. McGlashan and D. J. B. Potter, *Proc. R. Soc. London, Ser. A*, **267**, 478 (1962).
(41) R. R. Dreisbach, *Adv. Chem. Ser.*, **No. 15** (1955); **No. 22** (1959).
(42) "Encyclopedia of Polymer Science and Technology", Vol. 15, Wiley-Interscience, New York, N.Y., 1971, p 618.
(43) J. Brandrup and E. H. Immergut, Ed., "Polymer Handbook", 2nd Ed, Wiley-Interscience, New York, N.Y., 1975.
(44) J. E. Guillet and M. Galin, *J. Polym. Sci., Polym. Lett., Ed.*, **11**, 233 (1973).
(45) Some representative flow and retention diagrams are included here and the figures of the remaining systems are deposited as supplementary material.

Flows of Flexible Polymer Solutions in Pores

S. Daoudi[1a] and F. Brochard*[1b]

Physique de la Matière Condensée, Collège de France, 75231 Paris Cédex 05, France, and Laboratoire de Physique des Solides, Université Paris-Sud, Centre d'Orsay, 91405 Orsay, France. *Received March 21, 1978*

ABSTRACT: We study the passage of flexible polymers in solution through pores (of diameter D smaller than the radius of gyration of the chains, R_F) driven by hydrodynamic flows through the pore (characterized by a current of the solvent, J_s). (1) For the case of slightly *conical* pores (first converging and then diverging) the chains are drawn in above a critical current J_c. For a dilute solution, $J_c \simeq J_{c_1}\epsilon$, where ϵ measures the angle of the cone and $J_{c_1} \simeq T/\eta_s$ depends only on the temperature T and the solvent viscosity η_s, but is independent of D and of the molecular weight (at large molecular weights). For a semidilute solution at the entrance of the pore, one finds three regimes depending upon the bulk concentration c_0, the minimal cross section, and the current's strength J_s: (α) a free flowing state of the SD solution throughout the pore, (β) a partially flowing state with a dilute region extending downstream from the minimal section, (γ) a clogged state where a dilute region is present both upstream and downstream. (2) For a capillary of *constant cross section* passing through a flat wall, the chains are subjected to an elongational flow at the entrance. Above a critical current $J_s = J_c'$, they are sufficiently stretched to enter the pore. For dilute solutions, $J_c' = J_{c_1}$. In semidilute solutions J_c' ought to vary as $C^{-15/4}$. We also discuss elongational effects at the entrance of macroscopic capillaries.

I. Introduction

Besides fundmental interest (polymers in one and two dimensions), the study of flexible polymer solutions trapped in porous media has important applications: in particular the extraction of oil from porous geological structures by injection of polymer solutions of high molecular weight. Practical situations always correspond to polymer solutions in good solvents: for this case, we have results concerning the partitioning and the dynamics of macromolecules confined in pores.[2] These two problems have been studied theoretically very recently by Daoud and de Gennes[5] (thermodynamic properties) and by Brochard and de Gennes[6] (diffusion and internal modes). In these studies the emphasis was placed on the behavior of chains in an immobile solvent. The corresponding experiments are rather difficult because of the small percentage of chains in pores of small diameter.

On the contrary, in all the experiments proposed here, one forces the polymer to penetrate into the pores by applying a solvent current J_s. We have considered two types of pores: (a) slightly conical pores (Figure 2), and (b) cylindrical pores with an entrance at which the flow is strongly convergent (Figure 8). In conical pores, the polymer is sucked in if the frictional force exerted by the solvent is sufficient to overcome the elastic forces resisting confinement. In pores of constant cross section, the process of penetration is due to the elongational shear which stretches the chain *before* its entrance. Case (a) is statistically realized by pores in porous media. Case (b) corresponds to commercially available structures (nucleopores in plexiglas have cylindrical geometries and diameters $D \gtrsim 150$ Å), or can be approximated by pores in leached glass[2] or with crystallographic structures such as zeolites ($D \gtrsim 20$ Å).

We assume that polymer adsorption on the solid surface is negligible. This can be achieved by treating the pores chemically.[2] We also restrict our attention to *flexible* uncharged polymers for which the statistical and dynamical properties in bulk solutions are now well described by scaling methods.[3,4]

Here also we use as a theoretical framework the techniques of scaling laws which are known to give good qualitative results, but all our results unfortunately lack exact numerical coefficients. In the first part, we review the equilibrium properties of confined chains for the two types of geometrics. In the second section we described the flow regimes of polymer solutions in conical pores (case a). In the third part, we study the effects of polymer accumulation and forced penetration at the entrance of cylindrical pores (case b).

0024-9297/78/2211-0751$01.00/0